ELSEVIER

On the fracture toughness of calcium aluminate cement–phenol resin composites

Y. Qiao*

Department of Civil Engineering, University of Akron, ASEC 210H, 244 Sumner Street, Akron, OH 44325-3905, USA

Abstract

Macro-defect-free (MDF) cement with high flexure strength has been an active research area over several decades. To study the tensile properties of these materials, it is essential to understand the mode I crack propagation. In this article, cleavage cracking in calcium aluminate cement (CAC)–phenol resin composites is analyzed based on an energy method. The crack-trapping effect of the cement particles is found to be significant. The fracture toughness rises with the particle size and is independent of the spacing between the particles. When the cement volume fraction is higher than a critical value the effective work of separation of the phenol resin decreases with the particle content with a coefficient of -1.88.

© 2004 Elsevier Ltd. All rights reserved.

Keywords: Fracture toughness; Tensile properties

1. Introduction

Macro-defect-free (MDF) cements have received great attention since early 1980s due to the excellent mechanical properties [1–3]. Associated with the decreasing of the porosity and the chemical reactions in the polymer phase involving ions released from cement particles [4], the flexural strength of MDF cements can be as high as that of structural steels [5,6]. Calcium aluminate cement (CAC) was found to be one of the best host cements. To produce the MDF cement, cement particles, plastisizers, polymers, such as poly(vinyl alcohol), phenol–formaldehyde resin, or nylon, as well as a small amount of solvent, such as water or methanol, should be combined in a low-shear planetary mixer and then roll-milled. Then the material is calendared into sheet and heat-treated to complete the polymerization process [3]. The MDF cement consists of the cement phase, the polymer phase, and the interphase. The interphase is formed through the reactions of the polymers and the hydration products. In the cement phase, the bulk material is partially anhydrous and could be partially replaced by other fillers [7,8].

MDF cements potentially have great applicability in structures where tensile stresses are significant. However, to implement these materials in engineering practice, the fracture behavior must be understood adequately. In an experimental study on CAC–phenol resin composites [9], it was found that, due to the strong CAC–phenol resin bonding, the fracture mostly occurred through the phenol resin matrix and the cement phase acted as reinforcing particles, as shown in Fig. 1 [9]. Although the phenol resin matrix was greatly toughened by the high-degree cross-linking through calcium and aluminum ions, the fracture mode was pure cleavage, resulting in the brittle behavior of the composites that fit well into the Griffith curve.

In a brittle matrix reinforced by well-bonded, tough particles, the crack-trapping effect of the particles causes additional resistance to cleavage cracking and the overall fracture toughness should increase with the particle content. However, experimental data [9] showed that in CAC–phenol resin composites, once the volume fraction of the cement particles, c, exceeds 60–70%, the flexural strength decreases significantly, which was attributed to that with high cement content the particles could not be fully lubricated.

To obtain the optimum mechanical properties and cost–performance balance, the cement content in MDF cements should be maximized. Understanding the cleavage-cracking

* Tel.: +1-330-972-2426; fax: +1-330-972-6020.
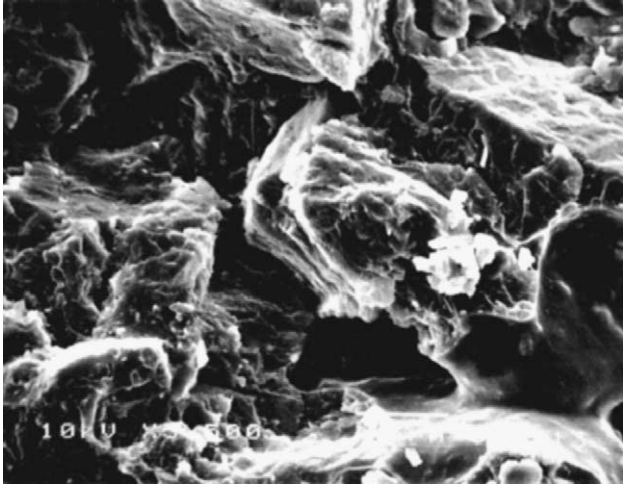*E-mail address:* yqiao@uakron.edu (Y. Qiao).

Fig. 1. SEM micrography of the fracture surface in a CAC–phenol resin composite [9].

behavior of these materials is of both basic scientific interest and immense technological importance. Currently, there is still no satisfactory model for the complicated crack-trapping effect of close packed hard particles. In this article, this phenomenon will be studied based on an energy method and the relationship between the fracture toughness and the cement content will be quantified.

2. Toughening effect of cement particles

In the brittle phenol resin matrix, the toughening effect of the cement particles is associated with both the additional work of separation and the crack-trapping effect. The cleavage front will be trapped locally when it encounters an array of cement particles. When the critical energy release rate G_{IC} is reached, the front will overcome the resistance offered by the particles and keep propagating unstably until it is arrested by the next array. If the cement content is relatively high, the particles are separated from the matrix before the front fully bypasses them, i.e., the separation occurs simultaneously with the onset of the unstable crack advance. Under this condition, the break-through processes at different particle arrays should be independent of each other. Neither the absence of the particles that the crack has already exposed nor the presence of the particles ahead of the crack front to be broken through has influence on the value of G_{IC}. Thus, in the following discussion, we will consider only one array of cement particles in the phenol resin matrix as depicted in Fig. 2.

To take account for the fact that the crack plane does not pass the main circle of each particle, the effective radius of particles exposed on the fracture surface, r, should be modified as [10]:

$$r = \sqrt{2/3}r_0 \approx 0.82r_0 \tag{1}$$

where r_0 is the actual particle radius. The volume fraction of the cement particles, c, is

$$c = \alpha\frac{(4/3)\pi r_0^3}{D^3} = \alpha\frac{4}{3}\left(\frac{3}{2}\right)^{3/2}\frac{\pi r^3}{D^3} \approx 7.69\alpha\frac{r^3}{D^3} \tag{2}$$

where α is a coefficient in the range of $1.0-1.91$ related to the particle shape and D is the center-to-center distance of the cement particles.

With the increasing of the nominal stress intensity at the crack tip, the crack front stably penetrates between the cement particles. When the critical penetration depth associated with G_{IC} is reached, the particles will be separated from the matrix and, since for reasons that will become clear G_{IC} is larger than the fracture resistance G_{pr} of the phenol resin matrix, the front will jump forward by a distance Δa, until the energy release rate decreases to G_{pr0}, the critical value for the matrix to arrest the propagating crack. Note that according to the experimental observations of dynamic crack advance [11], if the crack jump length Δa is smaller than the initial crack length a_0, the dynamic fracture resistance is about the same as the resistance to a stationary crack, i.e., $G_{pr0} \approx G_{pr}$. The validity of this assumption will be discussed shortly. During the breakthrough process, in addition to the work required to produce the fracture surfaces, significant work needs to be done to overcome the crack-trapping effect. Although this phenomenon has been studied intensively for low volume-fraction particles through the calculation of the sigmoidal crack front profile [12–16], there is still no satisfactory model that can be utilized to predict the front behavior across close-packed particles. It will be shown below that the critical stress intensity factor for the cleavage front to overcome a regular array of tough particles can be calculated through relatively simple energy analysis without simulating the detailed penetration process.

To calculate G_{IC}, consider the double cantilever beam (DCB) specimen depicted in Fig. 3. The major part of the specimen is homogenous phenol resin except for point "A" where the crack tip is trapped by a regular array of cement particles. With the increasing of the crack opening displacement, the energy release rate G_I rises. When $G_I = G_{IC}$, the
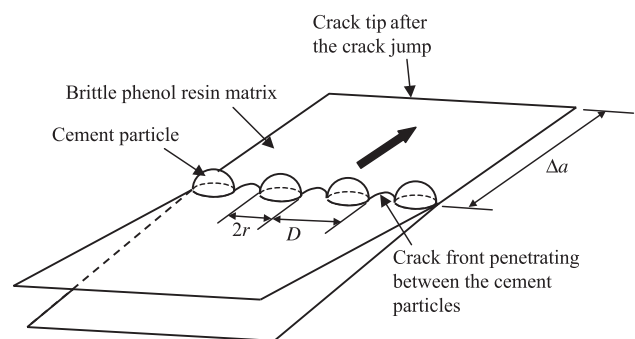

Fig. 2. A schematic diagram of the cleavage front overcoming the crack-trapping effect of a regular array of cement particles.
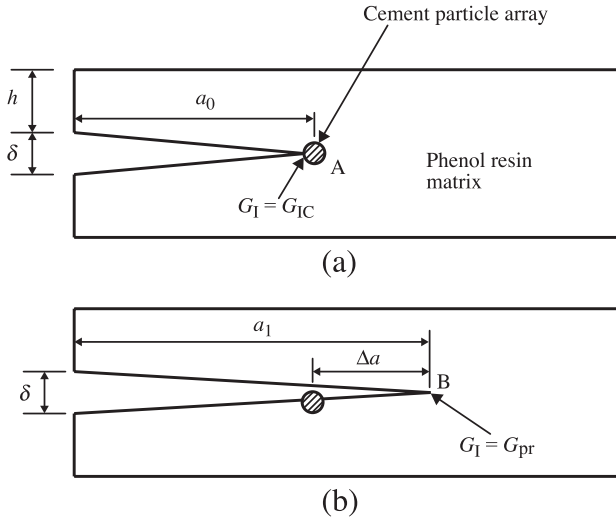
Fig. 3. Cleavage cracking in the DCB specimen: (a) before the crack breaks through the array of the cement particles; (b) after the crack jump.

crack breaks through the particle array and jumps to point "B" where G_I decreases to G_{pr}. During the crack jump, the crack opening displacement δ is assumed to be constant.

The strain energy U stored in the DCB specimen can be calculated as

$$U = \Gamma \frac{1}{a^3} \qquad (3)$$

where a is the crack length and $\Gamma = Ebh^3\delta^2/16$, with E being the Young's modulus of phenol resin, b being the specimen thickness, and h being the height of the DCB arms. Note that Eq. (3) is based on the basic beam theory. More accurate results can be obtained through modified beam theories or finite element method but since the influences of the shear stresses and the free edges are negligible the improvement should be below 3%. Through Eq. (3), the strain energy change associated with the crack jump is

$$\Delta U = \Gamma \left[\frac{1}{a_0^3} - \frac{1}{a_1^3} \right] \qquad (4)$$

where $a_1 = a_0 + \Delta a$. The total fracture work related to the crack jump is

$$W^* = bG_{pr}\Delta a + \frac{b}{D}\chi(2\pi r^2) \qquad (5)$$

where χ is the effective work of separation of unit area of the cement particles from the matrix. Note that according to energy conservation we have

$$\Delta U = W^* \qquad (6)$$

The energy release rate in the DCB specimen can be calculated through

$$G_I = -\frac{1}{b}\frac{\partial U}{\partial a} = \frac{3}{16}\frac{Eh^3}{a^4}\delta^2 \qquad (7)$$

Thus, according to the critical conditions, to break through the particle array and to stop the propagating crack in the matrix, we have

$$G_{IC} = \frac{3}{16}\frac{Eh^3}{a_0^4}\delta^2 \qquad (8a)$$

$$G_{pr} = \frac{3}{16}\frac{Eh^3}{a_0^4}\delta^2 \qquad (8b)$$

Consequently,

$$\frac{a_1}{a_0} = 1 + \frac{\Delta a}{a_0} = \tilde{G}^{1/4} \qquad (9)$$

where $\tilde{G} = G_{IC}/G_{pr}$, which can be rewritten as

$$\tilde{G} = \tilde{K}^2 \qquad (10)$$

where $\tilde{K} = K_{IC}/K_{pr}$, with K_{IC} and K_{pr} being the critical stress intensity factors to overcome the particle array and of the phenol resin matrix, respectively.

Finally, substituting Eqs. (4), (5), (8a), (9), and (10) into Eq. (6) gives

$$\tilde{K}^2 - 4\sqrt{\tilde{K}} = 3(W - 1) \qquad (11)$$

where

$$W = \frac{\chi(2\pi r^2)}{DG_{pr}a_0} \qquad (12)$$

Eq. (11) has the analytical solution

$$\tilde{K} = \sqrt{W + 2\sqrt{\frac{2}{3}W_0} + \frac{1}{2}\sqrt{W_1 + W_2 + W_3} - 3} \qquad (13)$$

where

$$W_0 = \frac{9 - 3W + \left(27 + 3\sqrt{3}\sqrt{W(27 - 9W + W^2)}\right)^{2/3}}{\left(27 + 3\sqrt{3}\sqrt{W(27 - 9W + W^2)}\right)^{1/3}}$$

$$W_1 = -\frac{32}{3^{2/3}}\left(9 + \sqrt{3}\sqrt{W(27 - 9W + W^2)}\right)^{1/3}$$

$$W_2 = \frac{32(W - 3)}{\left(27 + 3\sqrt{3}\sqrt{W(27 - 9W + W^2)}\right)^{1/3}}$$

$$W_3 = 64\sqrt{\frac{6\left(27 + 3\sqrt{3}\sqrt{W(27 - 9W + W^2)}\right)^{1/3}}{9 - 3W + \left(27 + 3\sqrt{3}\sqrt{W(27 - 9W + W^2)}\right)^{2/3}}}$$

Through Eq. (13), K_{IC} can be calculated quite conveniently if parameter W, which collects together both some well-known factors, such as r, D, a_0, and G_{pr}, as well as the somewhat ill-defined factor χ, is known. Note that W can be
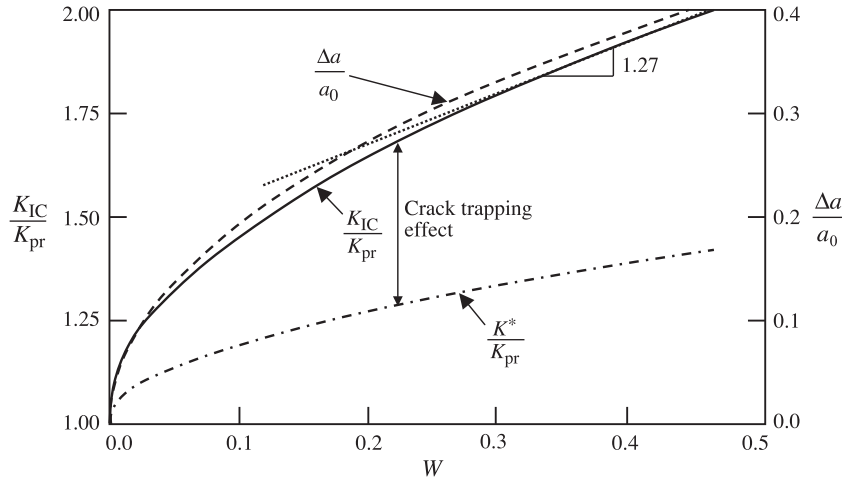
Fig. 4. The critical stress intensity factor and the crack jump length as functions of W.

considered as the effective fracture resistance of the particles, with both the crack-trapping effect and the work of separation being accounted for.

Fig. 4 shows that K_{IC} increases with W. When the value of W is relatively high, dK_{IC}/dW tends to a constant 1.27. Through Eq. (10), the crack jump length Δa can be obtained and the result is also shown in Fig. 4. It can be seen when W is in the range under consideration Δa is smaller than the initial crack length a_0, indicating that the above discussion is self-compatible.

3. Discussion

If we ignore the crack-trapping effect, the critical energy release rate of the composite can be estimated as

$$G^* = \frac{W^*}{\Delta a \cdot b} = \frac{\Delta U}{\Delta a \cdot b} \tag{14}$$

Substitution of Eqs. (4), (9), and (11) into Eq. (14) gives

$$\tilde{K}^* = \sqrt{\tilde{G}^*} = \sqrt{\frac{1}{3}\frac{\tilde{K}^2 - \tilde{K}^{1/2}}{\tilde{K}^{1/2} - 1}} \tag{15}$$

where $\tilde{G}^* = G^*/G_{pr}$ and $\tilde{K}^* = K^*/K_{pr}$, with K^* being the critical stress intensity factor with the crack-trapping effect being ignored. As shown in Fig. 4, K_{IC} is significantly larger than K^*. When W is above 0.1, the crack-trapping effect causes a 20–30% increase of the fracture toughness. The larger the W, the more pronounced the crack-trapping effect.

Although Eq. (11) was derived based on the discussion of the DCB specimen, the result of K_{IC} is independent of the specimen geometry and the loading condition. In a three-point bending experiment of CAC–phenol resin composites with various cement contents, Pushpalal [9] found that the flexure strength increases with the cement particle volume fraction, c, up to about 66% and then tends to drop. This critical volume fraction is related to the minimum amount of

resin required to fully lubricate the particles. Since in well-bonded composites if the particles were perfectly spherical the particle volume fraction cannot exceed 52.3%, the particle shape factor α in Eq. (2) should be taken as $\alpha = 66\%/52.3\% = 1.26$. According to the experimental data [9], when c is relatively high but still below 66%, $S_f \approx 7.5c + S_0$, where S_f is the flexure strength of the composites normalized by that of phenol resin and S_0 is a material constant. The compression strength of phenol resin is taken as 70 MPa. Note that the critical stress intensity factor at the tip of a microcrack at the bend-over-point (BOP) is linear to S_f. Consequently,

$$\tilde{K} \approx 7.5c + \tilde{K}_0 \tag{16}$$

with $\tilde{K}_0$ being a material constant.

Assume that initially the microcracks in the specimen are of the size comparable to the cement particles, i.e., $a_0 = 2r$. Thus, W can be rewritten as

$$W = \pi \frac{\chi}{G_{pr}} \frac{r}{D} \tag{17}$$

Through Eq. (11), when W is relatively large, $d\tilde{K}/d(W^3) \approx 2.17$. This relationship, together with Eqs. (2) and (17), leads to

$$\tilde{K} = 6.9(\chi/G_{pr})^3 c + \tilde{K}_0 \tag{18}$$

Comparison of the theoretical result Eq. (18) and the experimental result Eq. (16) gives

$$\chi/G_{pr} = 1.03, \tag{19}$$

i.e., the effective particle–matrix bonding strength is about the same as the strength of the matrix itself. This is compatible with the experimental observation that the debonding of the actual cement–phenol resin interface is quite difficult and the fracture mostly occurs through the matrix [9].

When the particle volume fraction exceeds about 66%, the flexure strength S_f decreases with c. Based on the experimental data [9], this relationship can be simplified as

$$\tilde{K} \approx -6.6c + \tilde{K}_1 \tag{20}$$

with $\tilde{K}_1$ being a material constant. Since the fracture occurs in the matrix, the decreasing of the overall flexure strength must be attributed to the imperfectness of the phenol resin. Comparison of Eq. (20) to Eqs. (16) and (18) shows that

$$\frac{\Delta\chi}{G_{pr}} = -1.88(c - 0.66) \tag{21}$$

with $\Delta\chi$ being the change of χ. The decrease in the phenol resin strength can be suppressed by using cement particles with bimodal size distribution.

Based on Eqs. (2) and (19), Eq. (12) can be rewritten as

$$W = 3.03 \cdot c^{1/3} \frac{r}{a_0}, \tag{22}$$

It can be seen that with constant particle volume fraction the particle size has significant influence on the value of W, which, in turn, affects the fracture toughness. With the increasing of the cement particle size, the crack-trapping effect becomes more important and, consequently, the composite is tougher. This is due to the non-self-similar nature of the crack front behavior when r varies.

According to Eq. (22), the fracture toughness of the CAC−phenol resin composite is not a material constant. The value of K_{IC} for longer cracks is smaller than that for smaller cracks. This phenomenon is quite similar to the crack length dependence in the well-known R curve analysis, where the change of the energy release rate $\partial^2 U/\partial a^2$ is dominant. In this model, the factor of $\partial^2 U/\partial a^2$ comes in by affecting the crack jump length since the problem is not scalable when the crack length varies while the particle size is constant. The longer the crack jumps after breaking through the particle array, the less significant the work of separation of the cement particles.

With the same cement content, changing the center-to-center distance of the cement particles has no influence on K_{IC}, unless the particle volume fraction exceeds 66% where the change of D can only be attributed to the change in the aspect ratio of the particles. However, as discussed above, under this condition, the imperfectness of the phenol resin matrix becomes dominant and the effect of D should be only secondary.

4. Conclusions

In this article, the fracture toughness of an important MDF cement, CAC−phenol resin composite, is studied through an energy analysis. The contribution of the cement particles to the overall fracture work consists of two parts:

the crack-trapping effect and the geometrically necessary increase in the fracture surface roughness. Since in the energy analysis the simulation of the detailed crack front profile is avoided, the result is valid even when the particles are close packed. The following conclusions are drawn:

1. The fracture toughness of CAC−phenol resin composites is dominated by the effective particle fracture resistance, W, through $\tilde{K}^2 - 4\sqrt{\tilde{K}} = 3(W - 1)$.
2. The influence of the crack trapping on the cleavage crack advance is significant. About 20–30% of the toughness is due to the crack-trapping effect.
3. The effective cement−matrix bonding strength is about the same as that of the phenol resin. The fracture in the CAC−phenol resin composite mostly occurs through the phenol resin matrix and the cement particles serve as reinforcements.
4. If the particle volume fraction c is higher than 66%, the effective work of separation of the phenol resin decreases with c with a coefficient of −1.88.
5. With the same particle volume fraction, composites with coarse cement particles are tougher than composites with fine cement particles. This is not yet experimentally proved and will be studied in the future work.
6. The fracture toughness is crack length dependent. It is easier for longer cracks to overcome the crack-trapping effect of the cement particles.
7. With a constant particle volume fraction, the spacing between the cement particles does not have significant influence on the fracture toughness.

Acknowledgements

References

[1] R.N. Edmonds, A.J. Majumdar, The hydration of an aluminous cement with added polyvinyl alcohol-acetate, J. Mater. Sci. 24 (11) (1989) 3813–3818.
[2] G.K.D. Pushpalal, T. Kobayashi, M. Hasegawa, High alumina cement−phenol resin composite: water resistivity and effect of post hydration of unreacted cement on durability, Cem. Concr. Res. 27 (9) (1997) 1393–1405.
[3] G.K.D. Pushpalal, K. Kobayashi, T. Kawano, N. Maeda, The processing, properties, and applications of calcium aluminate−phenol resin composite, Cem. Concr. Res. 29 (1) (1999) 121–132.
[4] S.A. Rodger, S.A. Brooks, W. Sinclair, G.W. Groves, D.D. Double, High strength cement pastes. II. Reactions during setting, J. Mater. Sci. 20 (8) (1985) 2853–2860.
[5] J.D. Birchall, A.J. Howard, K. Kendall, Flexural strength and porosity of cements, Nature 289 (5796) (1981) 388–390.
[6] K. Kendall, A.J. Howard, J.D. Birchall, The Relationship Between Porosity, Microstructure, and Strength and the Approach to Advanced

Cement-Based Materials, ICI New Science Group, United Kingdom, 1983.

[7] J.F. Young, Recent advances in the development of high performance cement-based materials, in: K. Chong (Ed.), Materials for the New Millennium, ASCE, Reston, VA, 1996, p. 1101.

[8] S. Mindess, J.F. Young, D. Darwin, Concrete, Pearson Education, Upper Saddle River, NJ, 2002.

[9] G.K.D. Pushpalal, Fracture behavior of calcium aluminate–phenol resin composite, J. Mater. Sci. 35 (4) (2000) 981–987.

[10] F.A. McClintock, A.S. Argon, Mechanical Behavior of Materials, CBLS Publ., Marietta, OH, 1993.

[11] R.W. Hertzberg, Deformation and Fracture Mechanics of Engineering Materials, John Wiley & Sons, New York, 1976.

[12] H. Gao, J.R. Rice, A first-order perturbation analysis of crack trapping by arrays of obstacles, J. Appl. Mech. 56 (1989) 828–836.

[13] A.F. Bower, M. Ortiz, A three-dimensional analysis of crack trapping and bridging by tough particles, J. Mech. Phys. Solids 39 (6) (1991) 815–858.

[14] A.F. Bower, M. Ortiz, An analysis of crack trapping by residual stresses in brittle solids, J. Appl. Mech. 60 (1993) 175–182.

[15] T.M. Mower, A.S. Argon, Experimental investigations of crack trapping in brittle heterogeneous solids, Mech. Mater. 19 (1995) 343–364.

[16] G. Xu, A.F. Bower, M. Ortiz, The influence of crack trapping on the toughness of fiber reinforced composites, J. Mech. Phys. Solids 46 (10) (1998) 1815–1833.